Journal of Cell Science 108, 2747-2760 (1995)
Printed in Great Britain © The Company of Biologists Limited 1995

Guidance of oligodendrocytes and their progenitors by substratum topography

Anna Webb[1], Peter Clark[2], Jeremy Skepper[3], Alastair Compston[1,4] and Andrew Wood[1,*]

[1]Neurology Unit, University of Cambridge, Addenbrooke's Hospital, Hills Road, Cambridge CB2 2QQ, UK
[2]Department of Anatomy and Cell Biology, St Mary's Hospital Medical School, Norfolk Place, London W2 1PG, UK
[3]Multi-Imaging Centre, University of Cambridge, Downing Street, Cambridge CB2 3DY, UK
[4]MRC Cambridge Centre for Brain Repair, University Forvie Site, Robinson Way, Cambridge CB2 2PY, UK

*Author for correspondence at present address: CNS Disorders Division, Wyeth-Ayerst Research, 865 Ridge Road, Monmouth Junction, Princeton, NJ 08852, USA

SUMMARY

Oligodendrocyte progenitors arise in subventricular zones and migrate extensively during development before differentiating into mature oligodendrocytes, which myelinate nerve tracts in the central nervous system. We have used microfabricated substrata, containing periodic patterns of contours similar to those of central nervous system axons to assess the influence in vitro of substratum topography on oligodendrocytes isolated from 7 day rat optic nerve. Anti-ganglioside antibody A_2B_5 positive oligodendrocyte-type 2 astrocyte progenitors, and galactocerebroside positive and myelin basic protein positive oligodendrocytes, were highly aligned by surface contours as small as 100 nm depth and 260 nm repeat spacing. Rat optic nerve astrocytes also aligned on surface contours, but rat hippocampal and cerebellar neurons were unresponsive. Oligodendrocytes demonstrated enhanced parallel extension of their processes on narrow repeating topography in an arrangement similar to that found in the intact optic nerve. This is in marked contrast to the phenotype displayed by this cell type on planar substrata. Neither oligodendrocytes nor oligodendrocyte-type 2 astrocyte progenitors showed high-order F-actin cytoskeletal networks; thus their alignment on gratings is unlikely to result from deformation of actin cables and focal contacts. In contrast, aligned astrocytes showed striking arrangements of actin stress fibres. These results establish glial cells as potentially the most topographically sensitive cell types within the central nervous system. Furthermore, the topographical pattern inducing maximal alignment of oligodendrocyte lineage cells corresponds to the diameters of single axons within the 7 day optic nerve. Thus the migration of oligodendrocyte-type 2 astrocyte progenitors and axonal ensheathment by oligodendrocytes may be guided by axonal topography within the developing nerve.

Key words: microfabricated substratum, oligodendrocyte, O-2A progenitor, contact guidance, F-actin

INTRODUCTION

The migration of a number of cell types is influenced by fibrillar extracellular matrix (ECM) and oriented tissue structures. For instance, the spatial organisation of ECM fibrils in the embryonic axolotl trunk is implicated in directing neural crest cell migration (Lofberg et al., 1980); fibroblasts invading the primary corneal stroma of the chick embryo eye extend along collagen bundles in the posterior region of the stroma (Bard and Higginson, 1977); the highly ordered ECM of collagenous fibrils in the pectoral fin bud of the developing teleost embryo is strongly implicated in providing guidance cues to direct the migration of mesenchymal cells during skeletogenesis (Wood and Thorogood, 1984, 1987); and during neurogenesis many types of neuroblasts become oriented and migrate parallel to surrounding neurite bundles or glial fibres (Nagata and Nakatsuji, 1991; see review by Hatten, 1990). On the basis of these and in vitro studies (reviewed by Curtis and Clark, 1990; Dunn, 1982) fibrillar substratum anisotropy is thought to influence directed cell movements during tissue morphogenesis and pattern formation. However, to understand these influences it is crucial to identify which particular physical, chemical or mechanical aspects of the substratum are responsible for imparting guidance cues.

Oligodendrocyte progenitors undergo extensive migration during normal development, as demonstrated by transplantation and lineage tracing in the central nervous system (CNS) (Fulton et al., 1992; Gansmuller et al., 1991; Levison and Goldman, 1993; Pringle and Richardson, 1993; Warf et al., 1991; Warrington et al., 1993). These cells originate within subventricular zones (Levinson and Goldman, 1993) and in the case of the rat optic nerve, migrate from the chiasm to the retina along an established axonal fibre tract (Small et al., 1987), which provides a migration substratum consisting of parallel, aligned axons (Colello et al., 1994). On reaching their final destinations oligodendrocyte progenitors differentiate, ensheathe and myelinate single axons within fascicles. Development of the oligodendrocyte lineage is highly regulated (Barres et al., 1992; Barres and Raff, 1994) and it seems likely that environmental factors control the production of the highly stereotypi-

cal pattern of axonal myelin ensheathment which characterises CNS white matter.

In the intact optic nerve, oligodendrocyte progenitors and oligodendrocytes are surrounded by topographical and potentially complex chemical and mechanical cues, all of which may impart guidance information. Indeed, in vitro, oligodendrocyte-type 2 astrocyte (O-2A) progenitors are highly motile (Jacque et al., 1992; Small et al., 1987; Wolf et al., 1986); their movement can be influenced by discontinuities in substratum adhesiveness (Kiernan and ffrench-Constant, 1993) and by diffusible chemotactic gradients (Armstrong et al., 1990). To determine whether substratum topography influences oligodendrocyte lineage pathfinding, a series of micro- and nano-order gratings were used to investigate the response of cells to topography in the absence of chemical or mechanical heterogeneity (Brunette, 1986; Clark et al., 1987, 1990, 1991; Dunn and Brown, 1986; Wood, 1988). Additionally, since neuronal growth cones are considered to be extremely sensitive pathfinding organs of cell extension, we compared the in vitro topographical sensitivity of the rat oligodendrocyte lineage with rat hippocampal and cerebellar neurons.

MATERIALS AND METHODS

Microfabricated quartz substrata

Two types of microfabricated substrata etched onto chrome-plated quartz discs were used: those in which the dimensions of the topographical contours were of the order of micrometres, and ultrafine gratings in which the dimensions of the topographical contours were of nanometre size. The micrometre patterned substrata were produced by a modification of the processes used to make integrated circuits as described by Wood (1988). This method produced etched substrata consisting of an array of six 3 mm × 3 mm square areas, patterned with regular and parallel grooves of consistent dimensions. The ultrafine gratings were produced by a modification of a laser holographic method used to define masks for X-ray printing (Clark et al., 1991) and manufactured in quartz as described above for the micrometre patterns. The dimensions for the groove widths and depths of all the patterns used are shown in Table 1. Prior to cell culture, all discs were acid washed in a 7:1 (v/v) sulphuric acid:hydrogen peroxide solution. The discs were then rinsed thoroughly in distilled water before sterilisation in absolute ethanol. All discs were coated in poly-D-lysine (0.01% in sterile MilliQ water, Sigma) before cell plating.

Glial cell culture

Primary glial cultures were obtained from two sources: 7-day-old Sprague-Dawley rat neonatal optic nerves as described by Raff et al. (1983) and whole brains of 1- to 2-day-old Sprague-Dawley rats as described by McCarthy and de Vellis (1980). Glial cells from both the optic nerve and whole brain preparations were plated in N2B3 medium, as described by Bottenstein and Sato (1979), containing 0.5% foetal bovine serum (FBS) onto the microfabricated quartz discs (precoated with 0.01% poly-D-lysine) at a density of approximately 8×10^5 cells/ml (100 μl/disc) and incubated at 37°C in 5% CO_2.

Neuronal cell culture

Cerebellar granule cells were obtained from 8-day-old Sprague-Dawley rats as described by Levi et al. (1989), plated onto poly-D-lysine (0.01%)-coated microfabricated quartz discs at a density of 1×10^6 cells/ml and incubated in Dulbecco's modified Eagle's medium (DMEM) containing 10% FBS, overnight at 37°C in 5% CO_2. The following day the medium was replaced and supplemented with cytosine β-D-arabinofuranoside to a concentration of 10 μM.

Hippocampal neurons were obtained from E18 Sprague-Dawley rats. An E18 rat was killed by cervical dislocation and decapitation, the whole uterus was removed and placed in Krebs Ringer Buffer (KRB): 121 mM NaCl, 4.8 mM KCl, 1.25 mM KH_2PO_4, 25.5 mM $NaHCO_3$, 14.3 mM glucose and 45 μM Phenol Red. The embryos were removed from the uterus and decapitated immediately. The embryo heads were placed in fresh KRB, the meninges removed and the hippocampus was dissected out and placed into fresh KRB. The hippocampus was cut into 5-6 pieces, suspended in 10 ml trypsin solution (2.5 mg/10 ml in KRB) and incubated at 37°C in 5% CO_2 for 10 minutes, swirling occasionally. An equal volume of deoxyribonuclease solution (7.5 mg/10 ml deoxyribonuclease I in culture medium: 60% DMEM, 29% Ham's F12, 10% horse serum, 5 mM KCl, 2 mM glutamine and 1% penicillin/streptomycin) was added. Following centrifugation the tissue was resuspended in 1 ml of culture medium and triturated using a 1 ml plastic Gilson pipette tip. The cell suspension was filtered through a cell strainer, washed with more culture medium, made up to a volume of 3 ml and plated out onto poly-D-lysine (0.01%)-coated microfabricated quartz substrata at a density of 1×10^6 cells/ml.

Immunofluorescence

Filamentous actin was visualised in O-2A progenitor cells, oligodendrocytes and astrocytes cultured on microfabricated substrata by rhodamine-phalloidin (Sigma) using a staining protocol described by Rinnerthaler et al. (1988). Cells were rinsed briefly in 0.5% FBS-containing medium, followed by a rinse in a buffer designed to preserve cytoskeletal morphology (cytoskeletal buffer). This buffer contained 137 mM NaCl, 5 mM KCl, 1 mM Na_2HPO_4, 0.4 mM KH_2PO_4, 5.5 mM glucose, 4 mM $NaHCO_3$, 2 mM $MgCl_2(6H_2O)$, 2 mM EGTA and 10 mM MES, pH 6.1. The cells were subsequently fixed and permeabilised in cytoskeletal buffer with 0.5% Triton X-100 and 0.25% glutaraldehyde for 2 minutes at room temperature, followed by a further fixation in cytoskeletal buffer with 1% glutaraldehyde for 10 minutes at room temperature. Following fixation and permeabilisation, coverslips were treated with sodium borohydride (0.5 mg/ml) in cytoskeletal buffer (3× 5 minutes at 4°C) to reduce free aldehyde groups. Subsequently, cells were treated with 10% goat serum for 15 minutes at room temperature before incubation with rhodamine-phalloidin (500 nM) for 40 minutes at room temperature. Tubulin was visualised by using an antibody against β-tubulin (1:200, mouse monoclonal, Sigma) followed by fluorescein-conjugated anti-mouse IgG (1:100, Sigma).

Following visualisation of F-actin and beta-tubulin, cells cultured on microfabricated culture substrata were labelled with fluorescent markers to identify each specific glial cell or neuronal cell type. O-2A progenitor cells and immature oligodendrocytes were immunolabelled with A_2B_5 (mouse monoclonal; Eisenbarth et al., 1982) and a rabbit polyclonal to glial fibrillary acidic protein (GFAP; Dakopatts). Mature, fully differentiated oligodendrocytes were immunolabelled with a mouse monoclonal antibody to galactocerebroside (GalC; Ranscht et al., 1982) and a rat monoclonal antibody to myelin basic protein (MBP; Serotec). For immunolabelling of surface markers, cells were incubated at 37°C in primary antibody for 20 minutes, washed and incubated in secondary antibody for a further 20 minutes. The secondary antibodies used were fluorescein (anti-mouse, anti-rabbit and anti-rat) and rhodamine (anti-mouse and anti-rabbit). Primary antibodies were used according to the manufacturers' instructions and all secondary antibodies were used at a working dilution of 1:100. After incubation with antibodies the cells were mounted in Vectashield and viewed using both a Zeiss LSCM (laser scanning confocal microscope), by kind permission of Zeiss, Welwyn Garden City, and a Zeiss Axiovert 135 conventional epifluorescence microscope.

Determination of P7 optic nerve axon diameters by transmission electron microscopy

P7 rat pups were terminally anaesthetised with an intraperitoneal injection of sodium pentobarbitone. The thorax was opened and perfusion was initiated by inserting a 28 gauge needle into the left

ventricle. Fluid was drained by making an incision in the right atrium. The pups were exsanguinated by perfusion with 5 ml of physiological saline containing 2.5% polyvinylpyrolidine with a formula weight of 40,000 (PVP-40) maintained at 20°C and pH 7.4. This was followed by perfusion with 20 ml of 3% glutaraldehyde in 0.1 M PIPES buffer containing 2.5% PVP-40 and a final concentration of 2 mM $CaCl_2$. The fixative was maintained at a temperature of 4°C and pH 7.4. Hydrogen peroxide was added immediately before perfusion with fixative to a final concentration of 0.1% (Perracchia and Mittler, 1972).

The optic nerve and chiasm were dissected free and fixed by immersion for a further 4 hours in fresh fixative at 4°C. Three segments of nerve were removed for analysis, one adjacent to the retina, one adjacent to the chiasm and one midway between the two. These were rinsed twice in 0.1 M PIPES buffer containing 0.15% potassium ferricyanide (Karnovsky, 1971). The samples were rinsed twice in 0.1 M PIPES buffer followed by bulk staining with uranyl acetate. They were dehydrated in a series of ethanol solutions ascending to 100%, transferred to propylene oxide and embedded in Araldite. Ultrathin (<50 nm) transverse sections were cut using a Reichert Ultracut S, mounted on 300 mesh copper grids and double stained with uranyl acetate and lead citrate. The sections were viewed in a Philips EM 400 and a systematic random sampling routine (Weibel, 1979) was used to generate a sample of 10 micrographs/nerve cross-section. These were recorded at a magnification of ×10,000 and projected onto the digitising tablet of a Kontron Videoplan where the diameter of nerve axons was measured. The minimum diameter of each axon was measured to minimise errors arising from section obliquity. A minimum of 400 axon profiles was measured from each region.

Scanning electron microscopy

Glia cultured on the microfabricated substrata were examined by scanning electron microscopy (SEM). The culture medium was gently aspirated from the wells containing the quartz discs and replaced with the fixative as described in the previous section, but at 20°C. The samples were fixed for two hours and then dehydrated, as described previously, to 100% ethanol. They were then given two changes of Freon TF (Agar Scientific) and critical point dried. The quartz discs were mounted on aluminium stubs and coated with 20 nm of gold in a Polaron E5000 sputter coater before viewing in a JEOL JSM 35 scanning electron microscope operated at 15 kV.

Determination of cell alignment

Cells were examined under phase-contrast and fluorescence microscopy. A 180° eye-piece graticule (Graticules UK Ltd) was used to assess the alignment of each individual cell at ×400 or ×800 magnification. Where a less rigorous measure of process attitude (scored as aligning if within 45° of the longitudinal groove axis) was used this has been noted in the text. Process extension was calculated from photographic enlargements at ×2,500 by measuring transects at their point of origin from the soma to their distal tip with a transparent ruler calibrated in millimetres.

RESULTS

Oligodendroglial alignment by micrometre order topography

Cells of the oligodendroglial lineage were found to be highly aligned by topographical contours as visualised using confocal and conventional fluorescence microscopy. O-2A progenitors were identified as $A_2B_5^{+ve}$/$GFAP^{-ve}$ cells exhibiting a bipolar morphology. A small number of bipolar $A_2B_5^{+ve}$, $GFAP^{+ve}$ cells were obtained from both optic nerve and mixed brain cultures; these were assumed to be O-2A progenitors (see Wang et al., 1994) but were not included for analysis. Oligodendrocytes and O-2A progenitors from both optic nerve and cerebrum behaved identically on all gratings tested.

Fig. 1 illustrates the high degree of alignment exhibited by O-2A prtogenitors on various topographical substrata. Cells shown in Fig. 1A have been labelled with A_2B_5 (fluorescein) and phalloidin (rhodamine), which detects the cellular distribution of F-actin. The F-actin distribution in oligodendrocyte phenotypes appeared diffuse; however, phalloidin staining was useful in allowing us to visualise the full extent of very fine processes made by these cells. On topographical substrata O-2A progenitors and immature oligodendrocytes ($A_2B_5^{+ve}$, $GFAP^{-ve}$) adopted bipolar, multipolar and highly extended morphologies. In Fig. 1B a Nomarski DIC image has been transmitted in register with the fluorescence channels using confocal microscopy so that the underlying grooves (pattern G4/12) can be visualised. On wide gratings, $A_2B_5^{+ve}$ cells are able to bridge across inter-groove areas (inter-grooves are shown occurring between pairs of small white arrows). However, they are often constrained by the boundary between groove and inter-groove (cells 1,2 and 3 in A) or appear confined within single inter-grooves (cell 4 in A) or grooves (Fig. 1C). A small number of $A_2B_5^{+ve}$/$GFAP^{-ve}$ cells appeared completely refractory to the underlying pattern (cell 5 in A). Individual $A_2B_5^{+ve}$ cells demonstrated considerable process extension parallel to the longitudinal groove axis, either within the groove (see Fig. 1C; pattern A4) or constrained by the inter-groove area, especially on patterns with a periodicity below 8 μm. SEM analysis demonstrated that bipolar oligodendrocyte progenitors were able to spread on inter-grooves and groove surfaces (Fig. 1D; pattern A2G) and avoid groove surfaces by extending between closely adjacent inter-grooves (Fig. 1E; pattern A2R). Fig. 2A and B show bipolar $A_2B_5^{+ve}$ O-2A progenitors and multipolar $A_2B_5^{+ve}$ immature oligodendrocytes co-aligning on a pattern with narrow inter-grooves (groove, 1.5 μm; inter-groove, 1.3 μm; depth, 1.3 μm); most cell processes have apparently been deflected by their first encounter with a groove/inter-groove boundary, as shown at their point of origin with the cell soma (see cell 1 in B) and are subsequently constrained parallel to the pattern. Both $GalC^{+ve}$ (Fig. 2C,D; pattern A1) and MBP^{+ve} (Fig 2E,F; pattern A2R) oligodendrocytes demonstrated a degree of process alignment on most patterns with periodicities below 10 μm and depths between 0.8 and 1.2 μm. This alignment was normally confined to

Table 1. Mean pattern dimensions in micrometres

Pattern	Groove width	Inter-groove width	Groove depth
A1	0.98	1.03	1.17
A2G	1.93	1.17	1.14
A2R	1.43	1.81	1.14
A4	4.01	3.34	1.12
P1	0.13	0.13	0.10
P4	0.13	0.13	0.40
G2/4	2.0	4.0	0.75
G2/8	2.0	8.0	0.75
G4/12	4.0	2.0	0.75

peripheral processes only and the process network of the ‘skirt’ surrounding the soma and the larger processes emanating directly from it were non-aligned. This difference in response to topography may be controlled by process diameter, since processes derived directly from the soma are much thicker than their peripheral branches.

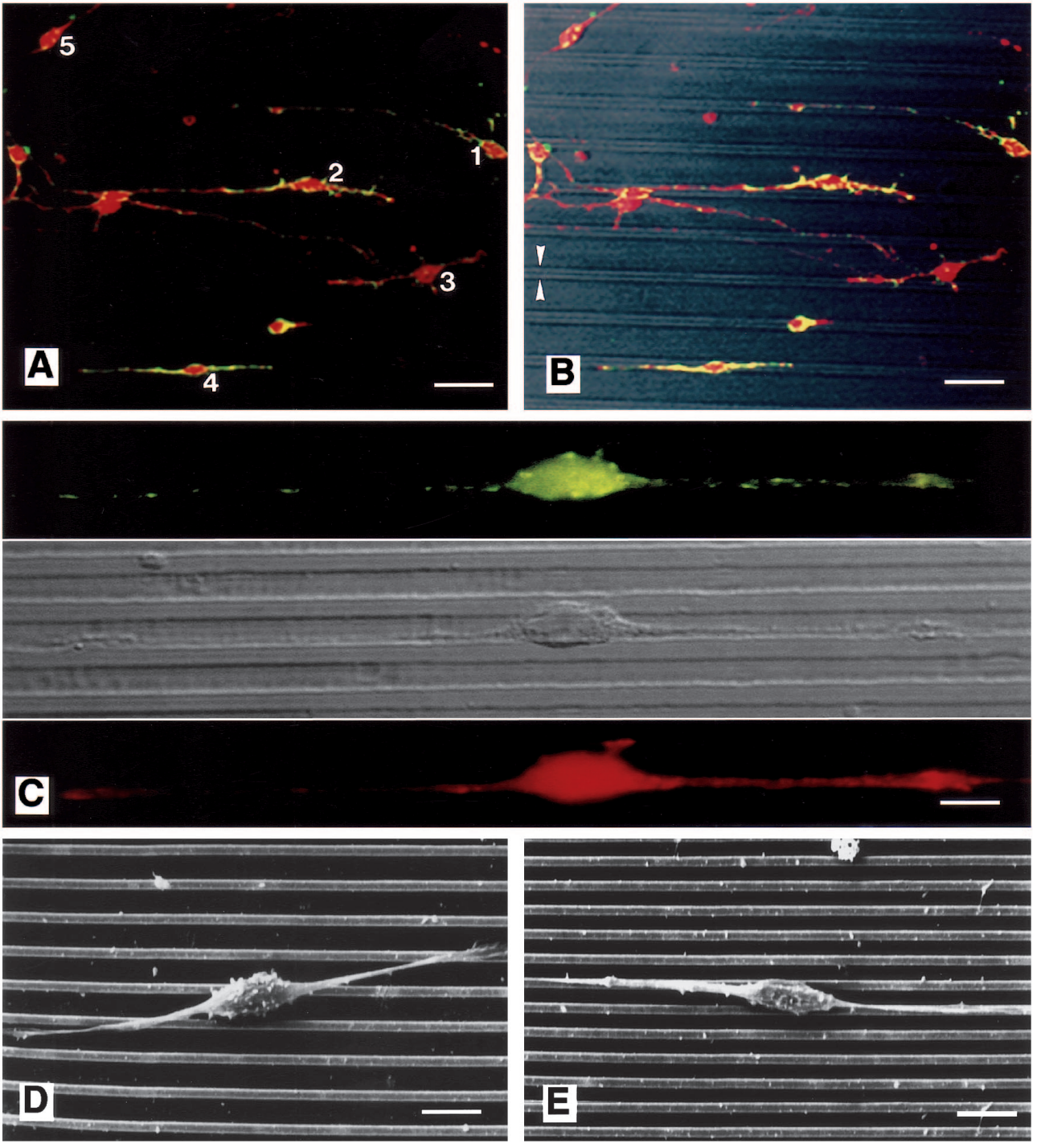

Fig. 1. Fluorescence and SEM photomicrographs of cell reaction to micrometre-order patterns etched in quartz. Cells are labelled with rhodamine-phalloidin and A_2B_5 (fluorescein). (A) and (B) O-2A progenitor cells cultured on pattern A4 observed under confocal fluorescence microscopy in the absence and presence of the groove structure, which has been transmitted through the fluorescent image in (B) using Nomarski DIC microscopy. (B) O-2A progenitor cells can be seen bridging across the grooves, aligning within grooves and against groove/inter-groove boundaries. (C) (pattern G4/12) A conventional fluorescence photomicrograph of a single O-2A progenitor cell aligning with the longitudinal groove axis under high magnification; notice that the cell’s bipolar process extension is aligned against the edge of the inter-groove boundary. (D) (A2G) and (E) (A2R) scanning electron micrographs of single O-2A progenitor cells cultured on grooved substrata; cells are able to bridge grooves and align their processes along narrow inter-groove contours. Bars: A and B, 25 μm; C, 5 μm; D and E, 10 μm.

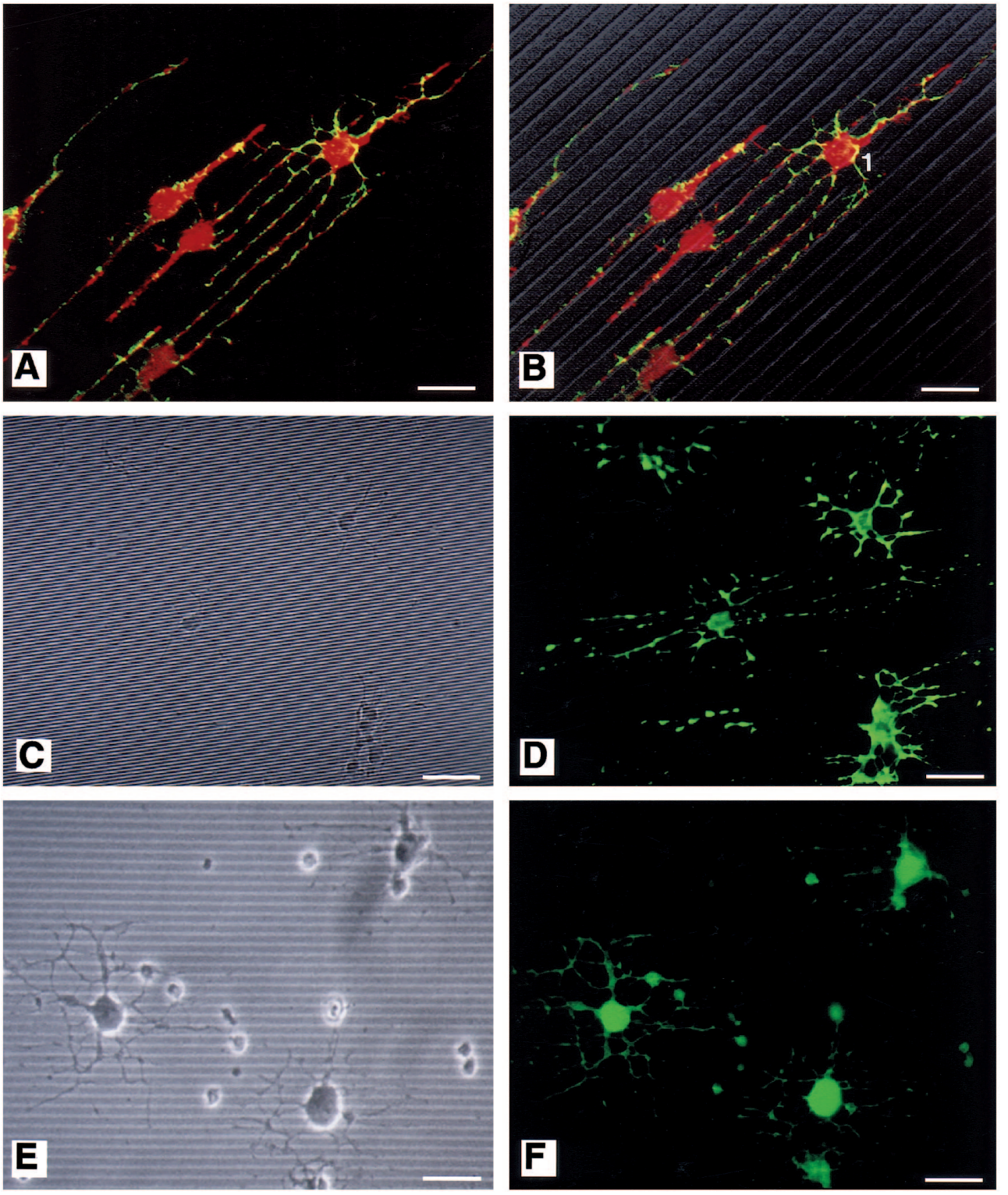

Fig. 2. Confocal and conventional fluorescence photomicrographs of cell reaction to micrometre-order patterns etched in quartz. (A and B) Highly aligned immature oligodendrocytes and O-2A progenitors cultured on grooved substrata (groove 1 μm; inter-groove 4 μm), the groove structure has been transmitted using Nomarski DIC microscopy through the confocal fluorescent image in (B); cells have been stained with A_2B_5 (fluorescein) and rhodamine-phalloidin. (C and D) (pattern A1) Phase-contrast and conventional fluorescent micrographs of oligodendroctyes (labelled with GalC) aligning on the grooved substrata. The phase-contrast image (C) gives a moiré grating pattern due to diffraction produced by the periodicity of the grooves; the longitudinal axis of the grooves is from the left to the right of the picture. (E and F) (pattern A2R) Phase-contrast and fluorescent micrographs of more mature oligodendrocytes (labelled with MBP) cultured on the grooved substrata. Secondary and tertiary processes can be seen to be aligning along the grooved surface. Double-headed arrows indicate groove direction. Bars: A and B, 20 μm; C, D, E and F, 25 μm.

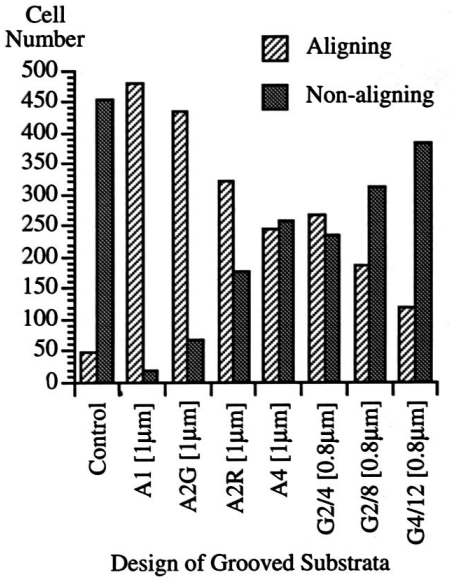

Fig. 3. Bar chart showing the distribution of O-2A progenitor cells on various gratings. Cells are scored as aligned if they conform to within 10° of the groove axis. Please refer to Table 1 for pattern definitions. Considerable cell alignment is produced by these patterns when compared with those on planar quartz.

Quantitation of oligodendrocyte and astrocyte alignment by micrometre order topography

Quantitation was carried out in two ways: Fig. 3 shows a quantitative assessment of the alignment of O-2A progenitors on various patterns to within 10° of the longitudinal axis of the grating and Table 2 presents orientation data for O-2A progenitors, oligodendrocytes and astrocytes, calculated by assessing process alignment For Fig. 3, a total of 500 cells were counted on each pattern; bipolar cells were scored as aligned if both processes extended parallel to the longitudinal grating for more than two-thirds of their length. $A_2B_5^{+ve}$, $GFAP^{-ve}$ tripolar cells were assumed to be immature oligodendrocytes and in most cases all processes of such tripolar cells were aligned on most patterns (data not included); $A_2B_5^{+ve}$ bipolar and tripolar cells with all other orientations were scored as non-aligned; cells with more than three processes were ignored. Grating A1 proved to be the most aligning pattern in the range above sub-micrometre periodicity and a decreasing number of cells aligned on patterns with increasing inter-groove and groove widths; all patterns scored a significant degree of cell alignment over planar substrata. Table 2 illustrates the alignment of cells to within 45° of the longitudinal axis. Use of this less rigorous criterion demonstrates that all topographies containing contours between 100 nm and 1200 nm are aligning to oligodendroglia, but unlike the data collected by scoring cells at 10° to the groove axis, alignment scored within 45° is less able to discriminate between effects generated by small differences in groove periodicity.

Response of developing oligodendrocytes to micrometre order topography

To determine whether the response of oligodendrocytes to topographical contours was developmentally regulated, the degree of alignment of the processes of mature oligodendrocytes (4 days in culture, MBP^{+ve}) was compared with that of processes from multipolar immature oligodendrocytes (1 day in culture, $A_2B_5^{+ve}$, $GFAP^{-ve}$), where alignment is defined as being within 10° of the grid axis. Oligodendrocytes have previously been classified as aligning if more than 50% of their processes were within 45° of the groove axis (see Table 2). However, as this designation was not sufficiently sensitive to distinguish differences in the guidance response of early and mature oligodendrocytes the actual number of aligning processes within 10° of the groove axis was recorded for each cell. Four topographical patterns were examined. In order of decreasing size these were: pattern A4, pattern A2R, pattern A2G and pattern A1. On the largest of the microfabricated patterns (A4) 51.4% (89/173) of processes from 10 MBP^{+ve} cells were classified as aligning, compared with 92.4% (61/66) of processes from 10 $A_2B_5^{+ve}$, $GFAP^{-ve}$ cells. On pattern A2R, 62.4% (166/266) of processes from 11 MBP^{+ve} cells were classified as aligning, compared with 90% (90/100) of processes from 11 $A_2B_5^{+ve}$, $GFAP^{-ve}$ cells. On pattern A2G, 70.5% (122/173) of processes from 11 MBP^{+ve} cells were classified as aligning, compared to 100% (71/71) of processes from 11 $A_2B_5^{+ve}$, $GFAP^{-ve}$ cells. On pattern A1, the smallest of the patterns examined in this study, 72.6% (159/219) of processes from 12 MBP^{+ve} cells were classified as aligning, compared with 97.8% (90/92) of processes from 12 $A_2B_5^{+ve}$, $GFAP^{-ve}$ cells.

Oligodendrocyte alignment by ultrafine topography

Two sub-micrometre topographical patterns were used: both patterns had a periodicty of 260 nm but had different groove depths of 100 and 400 nm (patterns P1 and P4, respectively).

Table 2. Glial cell orientation on grooved quartz substrata

Grooved substratum pattern	O-2A progenitors		Oligodendrocytes		Type I astrocytes		Type II astrocytes	
	Aligning	Non-aligning	Aligning	Non-aligning	Aligning	Non-aligning	Aligning	Non-aligning
Pattern A1	10	0	34	0	48	0	14	0
Pattern A2G	42	0	55	0	150	0	54	0
Pattern A2R	42	0	90	0	164	10	57	0
Pattern A4	62	2	44	4	143	3	43	0
Pattern P1	178	24	35	31	127	39	85	11
Pattern P4	163	8	126	5	185	6	223	25

Alignment of $A_2B_5^{+ve}$ O-2A progenitor cells has been assessed, as described, at 10°; $GalC^{+ve}$ or MBP^{+ve} oligodendrocytes and $GFAP^{+ve}$, $A_2B_5^{+ve}$ type 2 astrocytes were scored as aligned if more than 50% of their processes were within 45° of the groove axis; $A_2B_5^{-ve}$, $GFAP^{+ve}$ type 1 astrocytes were scored as aligned if the longitudinal axis of the cell was within 45° of the groove axis.

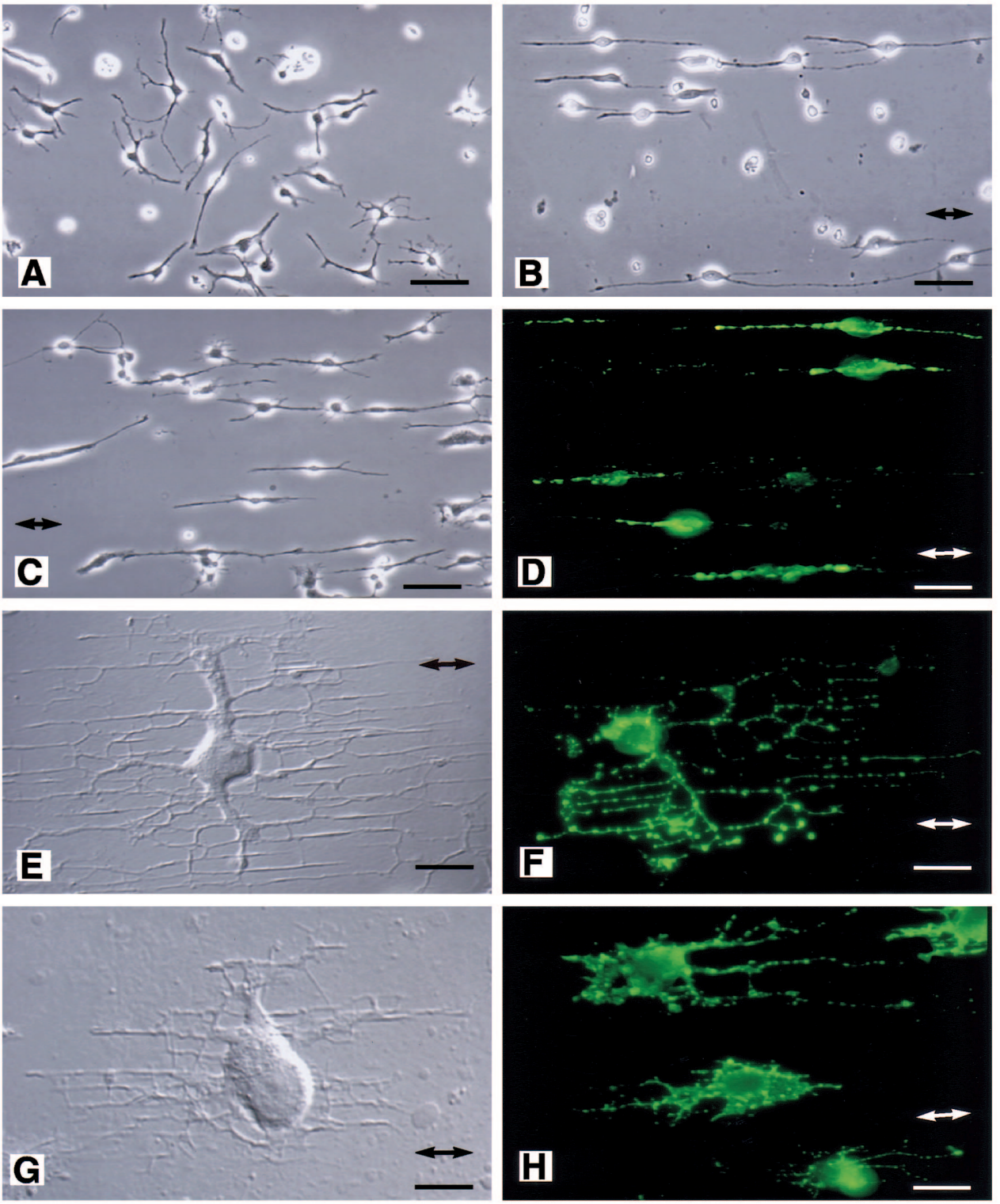

Fig. 4. Conventional fluorescence, phase-contrast and Nomarski DIC micrographs of O-2A progenitor cells and oligodendrocytes cultured on ultrafine sub-micrometre topographical gratings. (A) Phase-contrast control of O-2A progenitor cells on planar quartz adjacent to a patterned area. (B) Phase-contrast of O-2A progenitor cells on pattern P1; bi- and tri-polar cells are highly aligned. (C) Phase-contrast of O-2A progenitor cells on pattern P4; cells show a similar reaction to the deeper pattern. (D) Fluorescent micrograph of O-2A progenitor cells ($A_2B_5^{+ve}$ (fluorescein), $GFAP^{-ve}$ (rhodamine)) on pattern P1; N.B. different cells from those in C. (E) Nomarski DIC image of a single oligodendrocyte on pattern P4. (F) Fluorescent micrograph of an oligodendrocyte (labelled with GalC) on pattern P4; almost all fine processes are aligned with the longitudinal axis of the grating in E and F. (G) Nomarski DIC image of a single oligodendrocyte on pattern P1; this cell has less processes than the cell shown in E but they are similarly aligned by the shallower grating. (H) Fluorescent image of a more mature oligodendrocyte labelled with MBP on pattern P1. Double-headed arrows indicate groove direction. Bars: A, 50 μm; B and C, 30 μm; D, 25 μm; E, F and G, 10 μm; H, 25 μm.

It was not possible to resolve structural detail within the quartz sub-micrometre patterns, even with confocal microscopy. On both patterns there was extensive alignment of O-2A progenitors and oligodendrocytes. Fig. 4A and B demonstrate the extreme contrast in attitude between bi- and tri-polar phenotypes on planar (Fig. 4A) and patterned quartz (Fig. 4B; pattern P4). $A_2B_5^{+ve}$ cells were also aligned by pattern P1 (see Fig. 4C and D; note that cells depicted in C are different from those in D). The response of $GalC^{+ve}$ oligodendrocytes to sub-micrometre topography was striking. On planar substrata oligodendrocytes were highly arborised and extended many fine processes in radii from a central skirt of thicker cytoplasmic extensions from the soma. On patterns P1 and P4 almost all of the fine secondary or tertiary processes were aligned with the longitudinal axis of the grating; however, the thicker primary processes were refractory (see Fig. 4E and F). MBP^{+ve} oligodendrocytes were also strongly aligned by patterns P1 and P4.

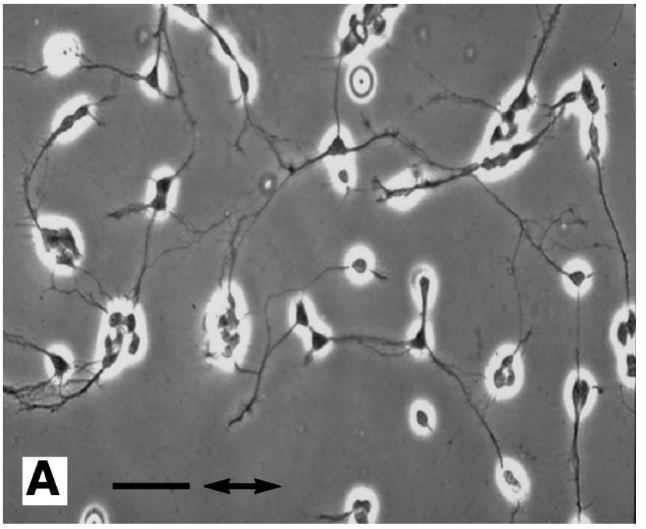

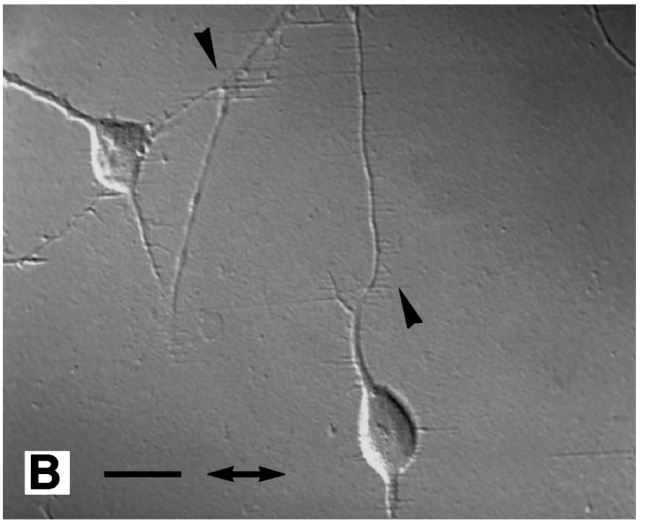

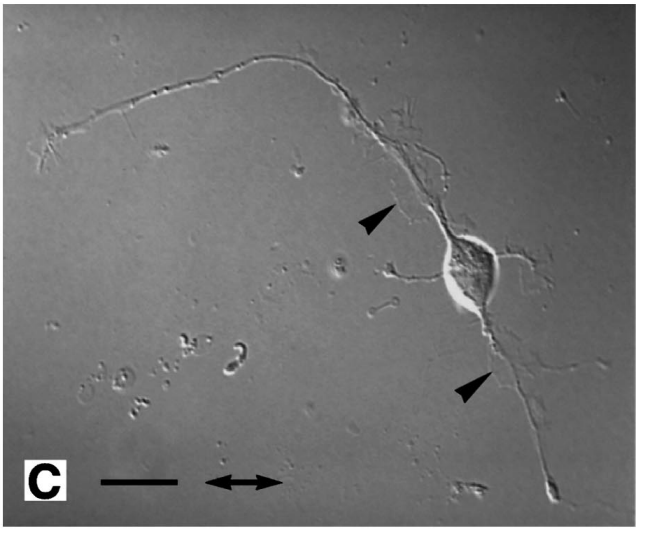

Fig. 5. Hippocampal and cerebellar granule cell neurons cultured on sub-micrometre gratings. (A) Phase-contrast of hippocampal neurons on pattern P1; hippocampal neurons are far less sensitive to the ultrafine surface contours than oligodendrocytes and their progenitors. (B) High magnification Nomarski DIC image of hippocampal neurons on pattern P4 (260 nm period, 400 nm deep grooves) shows alignment of small processes branching from the larger non-aligned processes (see arrowheads). (C) High magnification Nomarski DIC image of a cerebellar granule cell neuron on pattern P4; both processes emanating from the soma appear refractory to the grating. Double-headed arrows indicate groove direction. Bars: A, 30 μm; B and C, 10 μm.

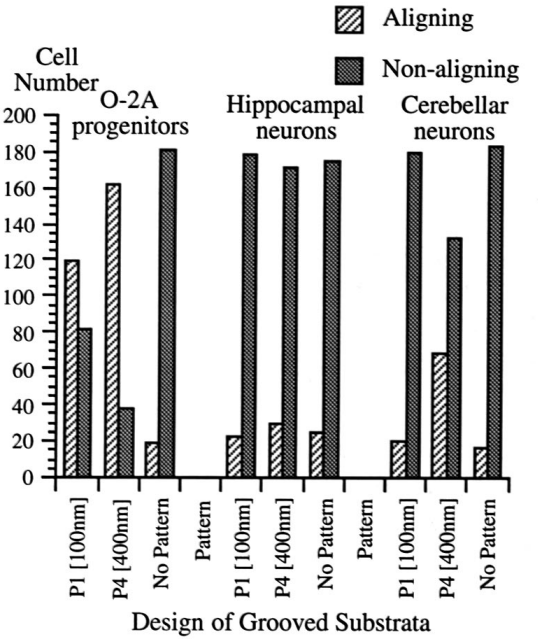

Fig. 6. Bar chart comparing the responses of O-2A progenitors, hippocampal neurons and cerebellar neurons to various gratings. Please refer to Table 1 for pattern definitions. O-2A progenitors are strongly aligned by both 100 nm and 400 nm deep gratings, whereas hippocampal neurons are insensitive and cerebellar neurons only respond to the 400 nm pattern; this response is transitory.

Neuronal alignment by ultrafine topography

In order to provide a comparison between the degree of sensitivity of neurons and oligodendrocyte lineage cells to topographical information, rat hippocampal and cerebellar neurons were also plated at low density onto patterns P1 and P4. Fig.

5A shows the behaviour of hippocampal neurons on pattern P1. Little cell or process alignment is detectable, producing alignment indices only slightly different from those achieved using planar quartz (see below). At higher magnifications, using Nomarski DIC microscopy, non-aligning hippocampal neurons displayed many fine processes, emanating from the extended non-aligned neurite, which spread for short distances along the longitudinal axis of the grating (see arrowheads in Fig. 5B). This was a common feature of this neuronal cell type on both 100 nm and 400 nm grating depths. In contrast to the hippocampal neurons, cerebellar neurons showed some alignment with the longitudinal axis of the P4 grating for up to 24 hours after plating (not illustrated). Within 24 hours, cells became refractory to the grating, without any obvious alteration to their bipolar morphology, and alignment with the pattern almost disappeared. Cerebellar neurons were not aligned by the P1 pattern and, unlike hippocampal neurons at high magnifications, fine process alignments were not detectable. Instead, skirts of flattened cytoplasm could be seen at the growth cones and surrounding neurites (see arrowheads in Fig. 5C).

Quantitative comparison of O-2A progenitor and neuronal alignment on ultrafine substrata

A quantitative measure of the difference in response to ultrafine gratings between glial and neuronal lineages was achieved by comparison of process alignment. 200 cells of each type were scored, as described previously (see Fig. 3). Fig. 6 illustrates that both cerebellar granule cells and hippocampal neurons showed no significant alignment response to a grating of 100 nm depth (P1). Hippocampal neurons were not aligned by the deeper grating of 400 nm (P4), but small numbers of cerebellar granule cells did conform to within 10° of the longitudinal axis of the grating. This alignment response was temporary and in contrast to bi- and tri-polar O-2A progenitor cells, which remained aligned by the grating.

Morphometric analysis of in vivo axonal topography

Fig. 7 illustrates the frequency distribution of unmyelinated axon diameters occurring in transverse TEM sections at three levels (chiasm, mid and retina) of proximo-distal section along a 7-day-old rat optic nerve. All sections demonstrated a wide distribution about a mean of approximately 0.19 micrometres (chiasm: 0.19, s.e.m. = 0.284; mid: 0.18, s.e.m. = 0.331; retina: 0.20, s.e.m. = 0.501). At least 400 axons were counted at each level. Small numbers of axons were bundled in groups, although most were discrete. Extracellular space and non-axonal cell processes were visible between axons. Very few myelinated axons were seen at any level, but those that were detected occurred predominantly at the retinal end, which is consistent with the retinal to chiasmal direction of myelination within the rat optic nerve (Fulton et al., 1992).

Cytoskeletal morphology and glial cell spreading

The cytoskeleton is associated with control of cell spreading and movement. We used the affinity of phalloidin for F-actin to study its distribution in O-2A progenitors, oligodendrocytes and astrocytes. Little high-order F-actin appeared to be present in oligodendroglia when visualised by confocal microscopy (resolution 0.2 μm). Fig. 8 shows the diffuse cytoplasmic distribution of F-actin observed in $A_2B_5^{+ve}$ bipolar cells. Oligodendrocytes did not appear to possess high-order F-actin organisation either, but did show complex microtubule arrays, as demonstrated by beta-tubulin staining (not illustrated), extending throughout the process network. Although tubulin was necessarily constrained to narrow aligned processes, individual tubules did not appear to be aligned in parallel with the groove axis. It is important to note that the determination of F-actin organisation in oligodendroglia is complicated by the small size of these cells and the thin calibre of their processes.

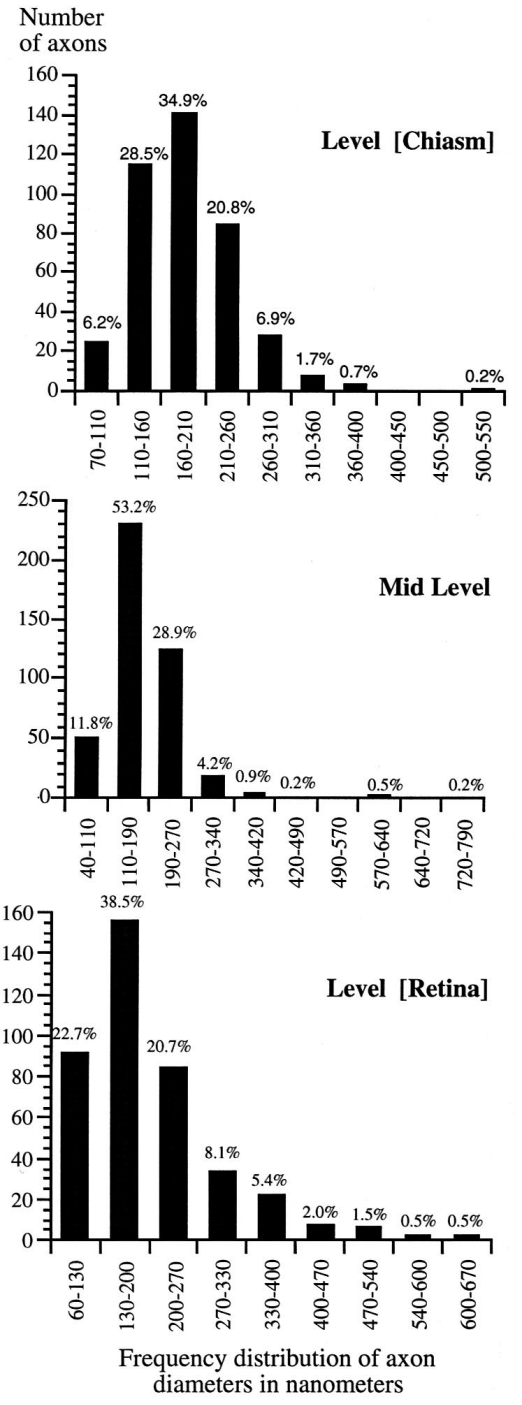

Fig. 7. The frequency distribution of axon diameters within the 7 day rat optic nerve at the optic chiasm, at a level mid-way between chiasm and retina, and at the level of the retina.

Thus, failure to detect high-order F-actin structure, without recourse to TEM, is not sufficient evidence for predicting that such structures do not exist in the oligodendrocyte lineage. However, phalloidin staining, visualised using conventional fluorescence microscopy, was sufficient to demonstrate actin cables in other, adjacent, cell phenotypes.

Fig. 9 shows a flattened astrocyte ($GFAP^{+ve}$, $A_2B_5^{-ve}$) process labelled with rhodamine-phalloidin. The extensive organisation of F-actin into 'cables' or 'stress fibres' is clearly visible (see Fig. 9B). Confocal 1.5 μm sections were taken through two transverse planes of section; these have been reconstructed and overlay the top of Fig. 9B (blue and green lines mark the transects). The distribution of actin cables (red and yellow fluorescence; yellow corresponds to peak intensity of rhodamine fluorescence emission) is clearly within the centre of the dorsi-ventral plane of cytoplasmic section. In Fig. 9A, a Nomarski DIC image has been transmitted through the fluorescent images and demonstrates co-alignment of the actin cables with the longitudinal axis of the grating. Similar alignments, seen in both other astrocytes and fibroblasts, were not consistent features across the entire cell, even when the processes were aligned. Where co-alignment of high-order F-actin structures was detectable, actin cables were aligned against groove/inter-groove boundaries (see Fig. 9A; red actin cables are partially overlain with diffuse green GFAP staining).

Although intermediate filament structure (GFAP) within flattened astrocytes was diffuse, some cells demonstrated a periodicity in distribution of GFAP co-incident with topographical features in the underlying pattern. Fig. 10A shows a periodicity approximating to the groove contours of pattern A4. The confocal reconstruction of 6 μm × 1.5 μm sections shown in Fig. 10B demonstrates that the greatest concentration of intermediate filaments is located centrally within the cell. Reconstruction from beneath the cell-substratum interface demonstrated that this cell was bridging grooves, but had also partially accommodated to the pattern by entering the upper margins of the groove; this corrugation of the underlying cell surface could cause the periodic pattern in GFAP staining.

DISCUSSION

This study has demonstrated the high degree of sensitivity of the oligodendrocyte lineage to topographical anisotropy. Both O-2A progenitors and oligodendrocytes were aligned by closely spaced micrometre-order contours, but as inter-groove spaces increased to several micrometres, both cell types became less aligned by the patterns. It is likely that the increased availability of planar surface area within patterns containing larger repeat spacings allows cell spreading perpendicular to grooves, and this behaviour, coupled with the ability of both cell types to bridge several widely spaced grooves, accounts for the observed decrease in alignment. On ultrafine, sub-micrometre gratings oligodendrocytes showed a

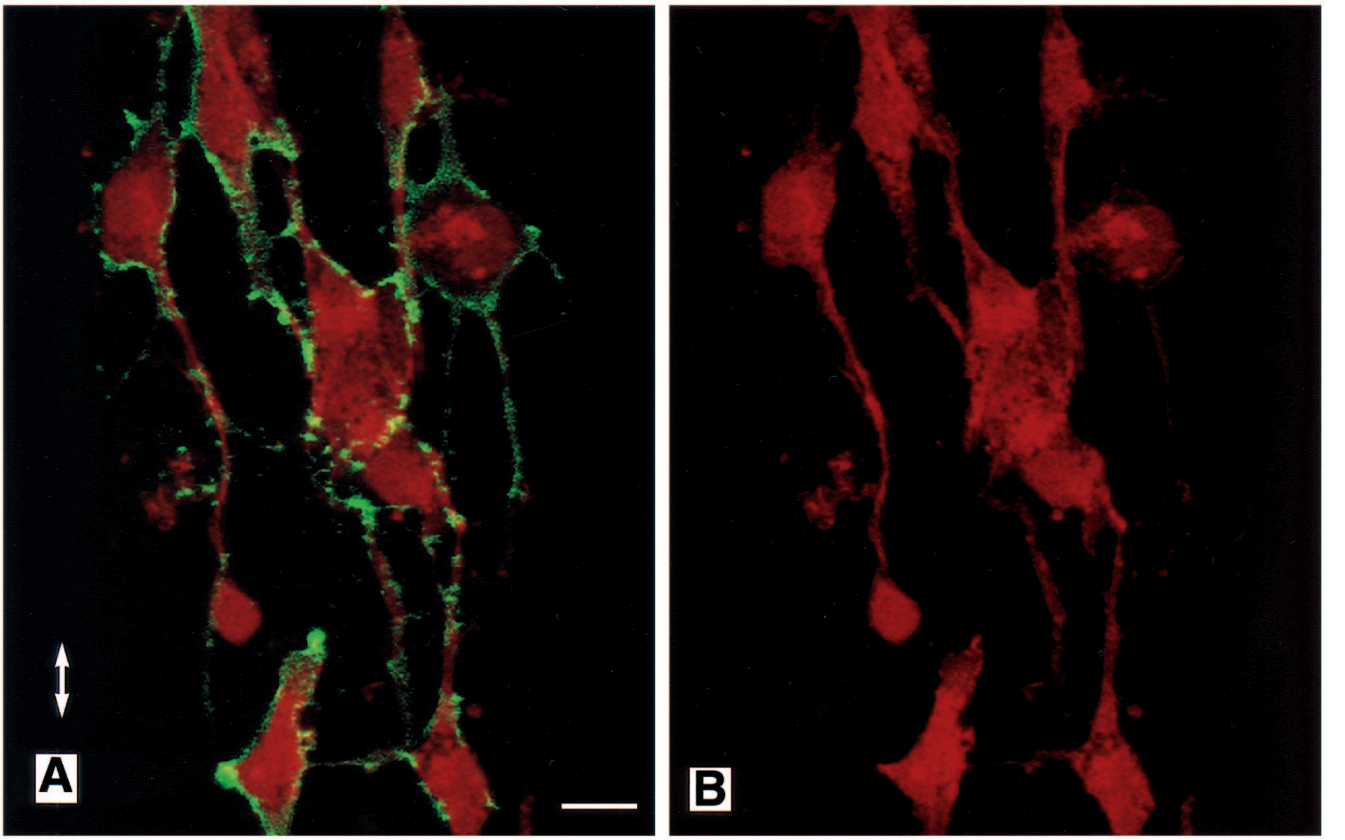

Fig. 8. Confocal photomicrographs of O-2A progenitor cells cultured on ultrafine, sub-micrometre gratings, labelled with rhodamine-phalloidin and A_2B_5 (fluorescein). (A) and (B) O-2A progenitor cells on pattern P4 (260 nm period, 400 nm deep grooves) with and without the fluorescein optics, respectively; the distribution of F-actin appears diffuse with no prominent fibres. Double-headed arrow indicates groove direction. Bars: A and B, 5 μm.

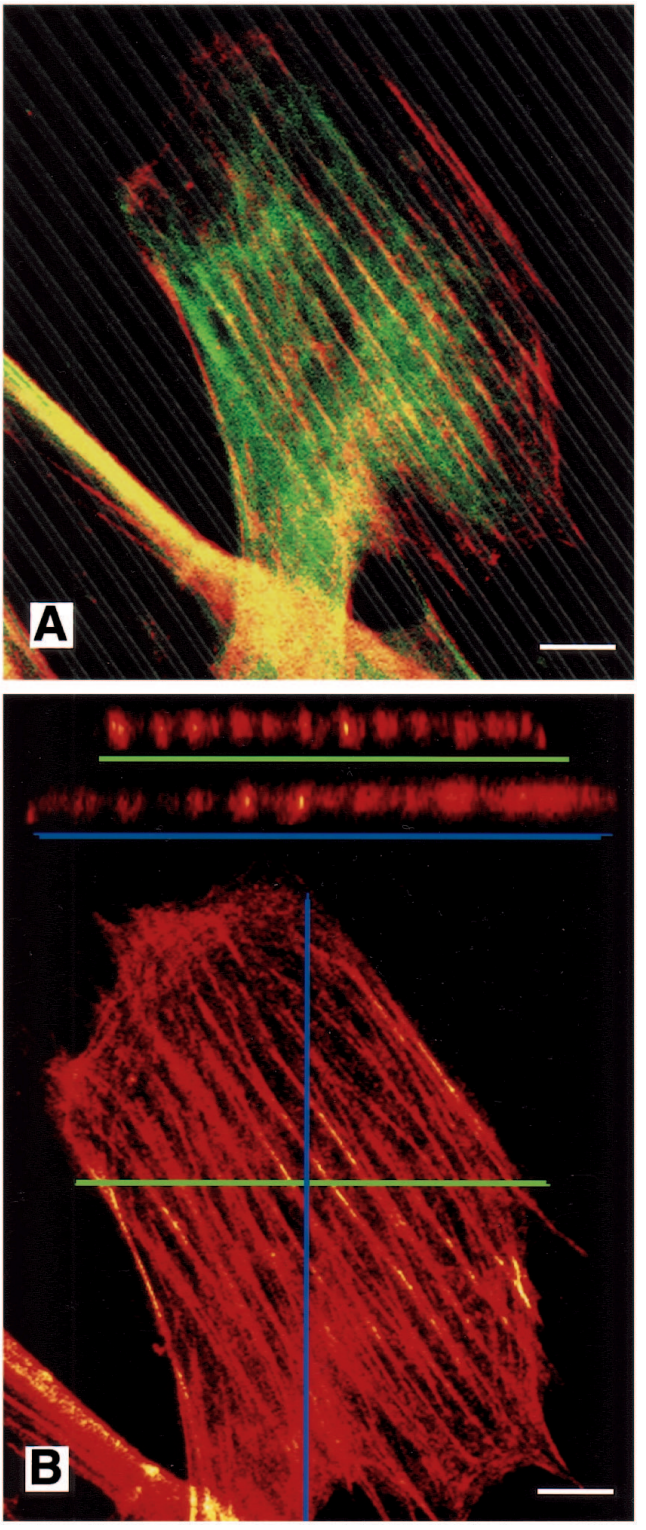

Fig. 9. Confocal fluorescent photomicrographs of an astrocyte process on pattern A2R labelled with rhodamine-phalloidin and fluorescein-visualised GFAP (A), illustrating the alignment of actin stress fibres along the longitudinal axis of the grooves. (B) The optical sectioning ability (6 sections taken at every 1.5 μm) of the confocal microscope was used to reconstruct a transverse section through the aligned actin stress fibres. Phalloidin staining was found throughout the depth of the cell, and not just at the cell-substratum interface. Bars: A and B, 10 μm.

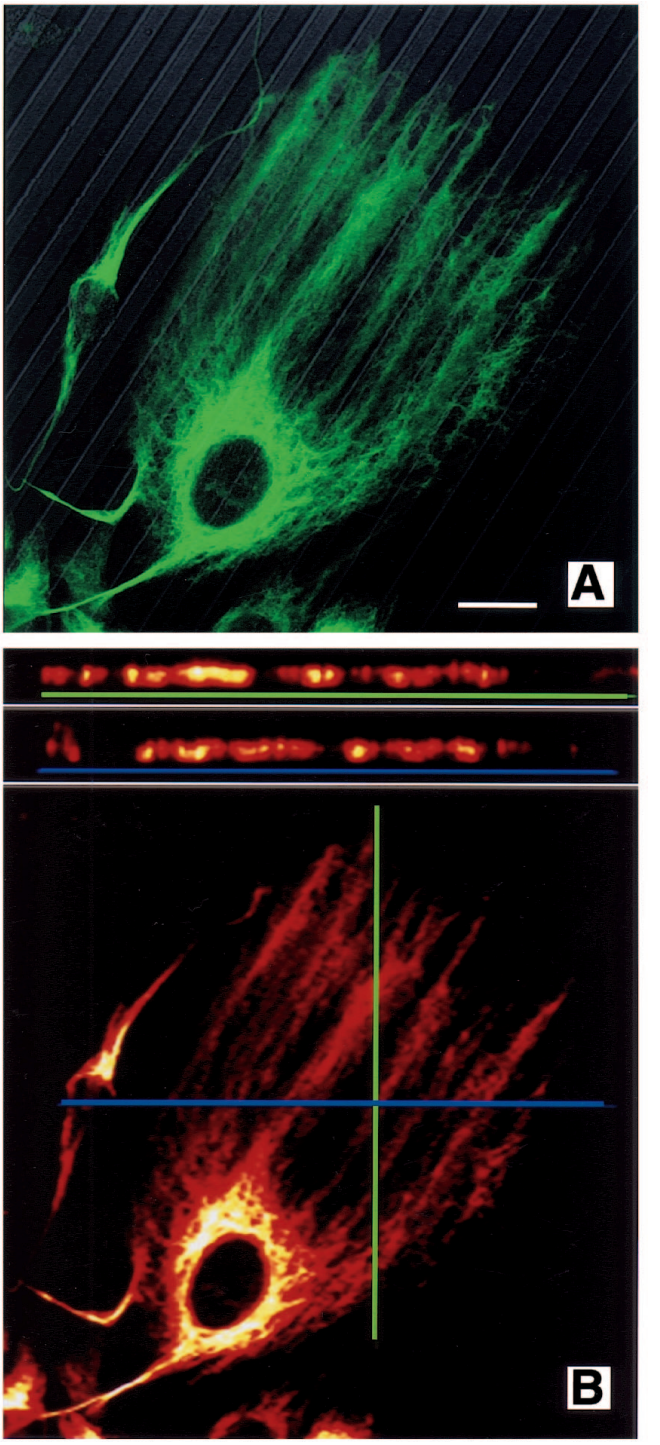

Fig. 10. Confocal fluorescent photomicrographs of an astrocyte on pattern A4 stained for GFAP (fluorescein) illustrating the alignment of bundles of GFAP intermediate filaments with the surface contours (A). (B) The cell was optically sectioned and reconstructed to demonstrate the location of intermediate filaments within the cytoplasm. Staining was not found at the substratum interface only, but was concentrated periodically throughout the cell. An undulating pattern in the upper and lower surfaces of the cell may be detected and may be consistent with unequal spreading, resulting in a concentration of cytoskeletal filaments over the inter-groove or groove areas. Bars: A and B, 15 μm.

striking phenotypic similarity with that displayed by their counterparts in the intact optic nerve (Butt and Ransom, 1993; Fulton et al., 1993) and quite unlike the radially arborised morphology adopted by these cells on planar substrata. Individual O-2A progenitors were also highly aligned by ultrafine grooves and, when plated in small clusters, migration was always greatest in parallel with the longitudinal axis of the grating (not illustrated). Although we were not able to test the threshold sensitivity of either cell type to surface contours (both O-2A progenitors and oligodendrocytes aligned on the finest pattern available: 100 nm depth, 260 nm period), these cells responded in vitro to gratings simulating the range of topographies presented by single axons within the 7 day rat optic nerve (see Fig. 7; and Colello et al., 1994).

The role played by glial cells in supporting neuronal cell migration is well established (Fishell and Hatten, 1991; Nagata and Nakatsuji, 1991; for reviews see Hatten, 1990; Poston et al., 1988). However, evidence is also accumulating that axons may act as guiding structures for glial cell migration (Giangrande, 1994; Kwang-Wook and Benzer, 1994). Although topographical sensing has not yet been unequivocally established as a mechanism underlying directed migration and morphogenesis during development, these in vitro data support the possibility that oligodendrocyte lineage cells utilise axonal topographical anisotropy in a number of ways during pathfinding and myelinogenesis. First, parallel alignment of the axonal migration substratum within the optic nerve could control migration of O-2A progenitors towards the retina by contact guidance; in addition to the bi-directional orientation imposed by the axonal architecture, chemical, mechanical or social influences (provided by groups of O-2A cells) could promote a uni-directional taxis. Indeed, since patterned surfaces can enhance the directional translocation and distribution of O-2A progenitors away from sites of high density (proliferation), this phenomenon may provide a potential mechanism to encourage grafted or injected cells across areas of severe tissue damage. Secondly, if individual axons and multiple fascicles present similar adhesive cues to oligodendrocytes (and there is no evidence to suggest otherwise), differences in axonal contours could provide a plausible mechanism to promote ensheathment of single fibres during myelination. Indeed, in vitro, oligodendrocytes are aligned by contours of 100 nm depth, suggesting that, in vivo, these cells could potentially detect the smallest calibre of axon on the basis of topography alone. Thirdly, since oligodendrocytes show increased parallel extension of their processes on patterned substrata, a similar mechanism operating in vivo might promote oligodendrocyte process extension along narrow axonal topography.

The mechanism by which astocytes are aligned can be described by the recently established F-actin cable-based hypotheses (Dunn and Heath, 1976; Ohara and Buck, 1979; Clark et al., 1991; Dunn, 1991). However, similar arguments cannot explain the alignment of some neurons and cells of the oligodendrocyte lineage on patterned substrata. The processes of neurons detect and respond to extrinsic cues that guide the direction of their extension. Indeed, the neuronal growth cone is considered archetypal in its ability to sense differences in chemical information. Chick cerebral neurons have been shown to be highly responsive to grooves of 8 μm period and 2 μm depth but unresponsive to ultrafine contours (Clark et al., 1990). In this study the processes of both rat cerebellar granule cell neurons and hippocampal neurons were also refractory to the ultrafine gratings of 100 nm depth, whereas oligodendrocyte lineage cells were highly aligned. This suggests that, in vivo, oligodendrocytes and their progenitors may use smaller topographical cues during pathfinding than those perceived by extending neurites. The lack of response shown by neurons to ultrafine gratings has previously been explained by their lack of high-order F-actin and focal adhesions. Their alignment by larger topographies is suggested to be mediated through smaller networks of actin filaments: Dunn (1991) also predicted that cells lacking focal contacts and actin cables are likely to be less sensitive to substratum shape.

It has recently been suggested that the high concentration of the actin-binding protein gelsolin in the oligodendrocyte lineage is responsible for the considerable motile ability of O-2A progenitors and extensive axonal ensheathment by oligodendrocytes (Tanaka and Sobue, 1994; Lena et al., 1994). Indeed, in fibroblasts, gelsolin usually localises to cytoplasm undergoing rapid protrusive activity (Cooper et al., 1988) and its overexpression in transfected NIH 3T3 fibroblasts produces enhanced motility. The enrichment of gelsolin in oligodendrocytes may cause rapid remodelling of the actin cytoskeleton and be incompatible with development of high-order actin cables, which might influence directional motility and spreading. Indeed, in this study and others (Kajikawa et al., 1991), actin cables are not detected in oligodendrocytes and O-2A progenitors (at least at the level of resolution of the confocal microscope) and yet these cells are still aligned by ultrafine gratings. This phenomenon currently presents a paradox to F-actin-based hypotheses explaining contact guidance; it will thus be important to examine further the actin cytoskeleton and precise interaction with the substratum at the ultrastructural level.

It is possible that more subtle mechanisms than constraint of high-order actin networks are responsible for cell guidance. For instance, surface contours may cause local restriction or redistribution of surface or integral membrane proteins (including ion channels), which may initiate a second messenger cascade, ultimately inducing cytoskeletal reorganisation and changes in motility. In fact, the cytoskeleton itself can regulate ion channel distribution; Levina et al. (1994) have demonstrated that local disruption of the cortical cytoskeleton in the growing tip of the oomycete, *Saprolegnia ferax*, alters the distribution of ion channels in the cell, provoking an intracellular signal cascade. As oligodendrocytes mature they become less aligned by the range of topographical contours used here. However, in mature MBP^{+ve} oligodendrocytes it was the thicker primary and secondary processes that were refractory to contours, whereas the finer tertiary processes still showed an alignment response. The large surface area to volume ratio experienced by fine tertiary processes might enhance their sensitivity to environmental stimuli compared to larger processes. Such sensitivity thresholding has been elegantly demonstrated in the filopodia that surround the growth cone of *Heliosma* neurons (Davenport et al., 1993).

Narrow period, multiple adhesive discontinuities have been shown to be ineffective at guiding neurite extension (Clark et al., 1993). If oligodendrocytes are also able to bridge small periods of adhesive discontinuity, the fine periodicity of chemical features created by the parallel array of axons in the optic nerve might be unable to align oligodendrocyte lineage

cells on the basis of adhesive heterogeneity alone. This study has demonstrated the potential of topographical anisotropy, of a similar order to that presented by optic nerve axons, to direct cell alignment and pathfinding of this lineage. In future studies it will be instructive to utilise similar in vitro approaches to investigate multiple guidance cues and to establish their hierarchy alone and in combination.

The work was supported by a MRC training award to Anna Webb. We thank Carl Zeiss UK for use of their laser scanning confocal microscope, and Graham Dunn, MRC Muscle and Cell Motility Unit, Kings College, London for use of patterns G2/4, G2/8, G4/12.

REFERENCES

Armstrong, R., Harvath, L. and Dubois-Dalcq, M. E. (1990). Type 1 Astrocytes and oligodendrocyte-type 2 astrocyte glial progenitors migrate towards distinct molecules. *J. Neurosci. Res.* **27**, 400-407.

Bard, J. B. L. and Higginson, K. (1977). Fibroblast-collagen interactions in the formation of the secondary stroma of the chick cornea. *J. Cell Biol.* **74**, 816-827.

Barres, B. A., Hart, I. K., Coles, H. S. R., Burne, J. F., Voyvodic, J. T., Richardson, W. D. and Raff, M. C. (1992). Cell death and control of cell survival in the oligodendrocyte lineage. *Cell* **70**, 31-46.

Barres, B. A. and Raff, M. C. (1994). Control of oligodendrocyte number in the developing rat optic nerve. *Neuron* **12**, 935-942.

Bottenstein, J. E. and Sato, G. H. (1979). Growth of a rat neuroblastoma cell line in serum free supplemented medium. *Proc. Nat. Acad. Sci. USA* **76**, 514-517.

Brunette, D. M. (1986). Fibroblasts on micromachined substrata orient hierarchically to grooves of different dimensions. *Exp. Cell Res.* **164**, 11-26.

Butt, A. M. and Ransom, B. R. (1993). Morphology of astrocytes and oligodendrocytes during development in the intact rat optic nerve. *J. Comp. Neurol.* **338**, 141-158.

Clark, P., Connolly, P., Curtis, A. S. G., Dow, J. A. T. and Wilkinson, C. D. W. (1987). Topographical control of cell behaviour: I. Simple step cues. *Development* **99**, 439-448.

Clark, P., Connolly, P., Curtis, A. S. G., Dow, J. A. T. and Wilkinson, C. D. W. (1990). Topographical control of cell behaviour: II. Multiple grooved substrata. *Development* **108**, 635-644.

Clark, P., Connolly, P., Curtis, A. S. G., Dow, J. A. T. and Wilkinson, C. D. W. (1991). Cell guidance by ultrafine topography in vitro. *J. Cell Sci.* **99**, 73-77.

Clark, P., Britland, S. and Connolly, P. (1993). Growth cone guidance and neuron morphology on micropatterned laminin surfaces. *J. Cell Sci.* **105**, 203-212.

Colello, R. J., Pott, U. and Schwab, M. E. (1994). The role of oligodendrocytes and myelin on axon maturation in the developing rat retinofugal pathway. *J. Neurosci.* **14**, 2594-2605.

Cooper, J. A., Loftus D. J., Frieden C., Bryan, J., Elson E. L. (1988). Localisation and mobility of gelsolin in cells. *J. Cell Biol.* **106**, 1229-1240.

Curtis, A. S. G. and Clark, P. (1990). The effects of topographic and mechanical properties of materials on cell behaviour. *Crit. Rev. Biocompatibility* **5**, 343-362.

Davenport, R. W., Dou, P., Rehder, V. and Kater, S. B. (1993). A sensory role for neuronal growth cone filopodia. *Nature* **361**, 721-724.

Dunn, G. A. and Heath, J. P. (1976). A new hypothesis of contact guidance in tissue cells. *Exp. Cell Res.* **101**, 1-14.

Dunn, G. A. (1982). Contact guidance of cultured tissue cells: a survey of potentially relevant properties of the substratum. In *Cell Behaviour* (ed. R. Bellairs, A. Curtis and G. Dunn), pp. 247-280. Cambridge University Press.

Dunn, G. A. and Brown, A. F. (1986). Alignment of fibroblasts on grooved surfaces described by simple geometric transformation. *J. Cell Sci.* **83**, 313-340.

Dunn, G. A. (1991). How do cells respond to ultrafine surface contours? *BioEssays* **13**, 541-543.

Eisenbarth, G. S., Walsh, F. S. and Nirenberg, M. (1979). Monoclonal antibody to a plasma membrane antigen of neurons. *Proc. Nat. Acad. Sci. USA* **76**, 4913-4917.

Fishell, G. and Hatten, M. E. (1991). Astrotactin provides a receptor system for CNS neuronal migration. *Development* **113**, 755-765.

Fulton, B. P., Burne, J. F. and Raff, M. C. (1992). Visualisation of O-2A progenitor cells in developing and adult rat optic nerve by quisqualate-stimulated cobalt. *J. Neurosci.* **12**, 4816-4833.

Gansmuller, A., Clerin, E., Kruger, F., Gumpel, M. and Lachapelle, F. (1991). Tracing transplanted oligodendrocytes during migration and maturation in the shiverer mouse brain. *Glia* **4**, 580-590.

Giangrande, A. (1994). Glia in the fly wing are clonally related to epithelial cells and use the nerve as a pathway for migration. *Development* **120**, 523-534.

Hatten, M. E. (1990). Riding the glial monorail: a common mechanism for glial guided neuronal migration in different regions of the developing brain. *Trends Neurosci.* **13**, 179-184.

Jacque, C., Quinonero, J., Collins, P. V., Villarroya, H. and Suard, I. (1992). Comparative migration and development of astroglial and oligodendrocyte cell populations from a brain xenograft. *J. Neurosci.* **12**, 3098-3106.

Kajikawa, D., Kubota, H., Mori, T., Shimo-oku, M. (1991). The distribution of actin on cultured oligodendrocytes from rat optic nerve. *Acta Soc. Opthalmol. Jpn* **95**, 944-950.

Karnovsky, M. J. (1971). Use of ferrocyanide-reduced osmium tetroxide in electron microscopy. *Proc. 14th Annu. Meet. Am. Soc. Cell. Biol.* pp. 146-149. Rockerfeller University Press, Baltimore, Maryland, USA.

Kiernan, B. W. and ffrench-Constant, C. (1993). Oligodendrocyte precursor (O-2A progenitor cell) migration; a model system for the study of cell migration in the developing central nervous system. *Development* supplement, 219-225.

Kwang-Wook, C. and Benzer, S. (1994). Migration of glia along photoreceptor axons in the developing Drosophila eye. *Neuron* **12**, 423-431.

Lena, J. Y., Legrand, CH., Faivre-Sarrailh, C., Sarlieve, L. L., Ferraz, C. and Rabie, A. (1994). High gelsolin content of developing oligidendrocytes. *Int. J. Dev. Neurosci.* **12**, 375-386.

Levi, G., Aloisi, F., Ciotti, M. T., Thangnipon, W., Kingsbury, A. and Balazs, R. (1989). Preparation of 98% pure cerebellar granule cell cultures. In *A Dissection and Tissue Culture Manual of the Nervous System* (ed. Shahar, de Vellis, Vernadakis and Haber), pp. 208-211. Alan R. Liss, New York.

Levina, N. N., Lew, R. R. and Brent Heath, I. (1994). Cytoskeletal regulation of ion channel distribution in the tip-growing organism *Saprolegnia ferax*. *J. Cell Sci.* **107**, 127-134.

Levison, S. W. and Goldman, J. E. (1993). Both oligodendrocytes and astrocytes develop from progenitors in the subventricular zone of postnatal rat forebrain. *Neuron* **10**, 201-212.

Lofberg, J., Ahlfors, K. and Fallstrom, C. (1980). Neural crest migration in relation to extracellular matrix organisation in the embryonic axolotl trunk. *Dev. Biol.* **75**, 148-167.

McCarthy, K. D. and de Vellis, J. (1980). Preparation of separate astroglial and oligodendrocyte cell cultures from rat cerebral tissue. *J. Cell Biol.* **85**, 890-902.

Nagata, I. and Nakatsuji, N. (1991). Rodent CNS neuroblasts exhibit both perpendicular and parallel contact guidance on the aligned parallel neurite bundle. *Development* **112**, 581-590.

Ohara, P. T. and Buck, R. C. (1979). Contact guidance *in vitro*. A light transmission and scanning electron microscopic study. *Exp. Cell Res.* **121**, 235-249.

Peracchia, C. and Mittler, B. S. (1972). Fixation by means of glutaraldehyde-hydrogen peroxide mixture. *J. Cell Biol.* **53**, 234-236.

Poston, M. R., Fredieu, J., Carney, P. R. and Silver, J. (1988). Roles of glia and neural crest cells in creating axon pathways and boundaries in the vertebrate central and peripheral nervous systems. In *The Making of the Nervous System* (ed. J. G. Parnavelas, C. D. Stern and R. V. Stirling). Oxford Scientific Publications, Oxford.

Pringle, N. P. and Richardson, W. D. (1993). A singularity of PDGF alpha-receptor expression in the dorsoventral axis of the neural tube may define the origin of the oligodendrocyte lineage. *Development* **117**, 525-523.

Raff, M. C., Miller, R. H. and Noble, M. (1983). A glial precursor that develops *in vitro* into an astrocyte or an oligodendrocyte depending on the culture medium. *Nature* **303**, 390-396.

Ranscht, B., Clapshaw, P. A., Price, J., Noble, M. and Seifert, W. (1982). Development of oligodendrocytes and Schwann cells studied with a monoclonal antibody against galactocerebroside. *Proc. Nat. Acad. Sci. USA* **79**, 2709-2713.

Rinnerthaler, G., Geiger, B. and Small, J. V. (1988). Contact formation

during fibroblast locomotion: involvement of membrane ruffles and microtubules. *J. Cell Biol.* **106**, 747-760.

Small, R. K., Riddle, P. and Noble, M. (1987). Evidence for the migration of oligodendrocyte-type 2 astrocyte progenitor cells into the developing rat optic nerve. *Nature* **328**, 155-157.

Tanaka, J. and Sobue, K. (1994). Localisation and characterisation of gelsolin in nervous tissues: gelsolin is specifically enriched in myelin-forming cells. *J. Neurosci.* **14**, 1038-1052.

Wang, C., Rougon, G. and Kiss, J. Z. (1994). Requirement of polysialic acid for the migration of the O-2A glial progenitor cell from neurohypophyseal explants. *J. Neurosci.* **14**, 4446-4457.

Warf, B., Fok-Seang, J. and Miller, R. H. (1991). Evidence for the ventral origin of oligodendrocyte precursors in the rat spinal cord. *J. Neurosci.* **11**, 2477-2488.

Warrington, A. E., Barbarese, E. and Pfeiffer, S. E. (1993). Differential myelinogenic capacity of specific developmental stages of the oligodendrocyte lineage upon transplantation into hypomyelinating hosts. *J. Neurosci. Res.* **34**, 1-13.

Weibel, E. R. (1979). Sampling of tissue. In *Stereological Methods* vol. 1, pp 63-91. Academic Press, New York.

Wolf, M. K., Brandenberg, M. C. and Billings-Gagliardi, S. (1986). Migration and myelination by adult glial cells: reconstructive analysis of tissue culture experiments. *J. Neurosci.* **6**, 3731-3738.

Wood, A. T. and Thorogood, P. (1984). An analysis of an in vivo cell migration during teleost fin morphogenesis. *J. Cell Sci.* **66**, 205-222.

Wood, A. T. and Thorogood, P. (1987). An ultrastructural and morphometric analysis of an in vivo contact guidance system. *Development* **101**, 363-381.

Wood, A. T. (1988). Contact guidance on microfabricated substrata: the response of teleost fin mesenchyme cells to repeating topographical patterns. *J. Cell Sci.* **90**, 667-681.

(Received 5 April 1995 - Accepted 23 May 1995)